metals

MDPI

Article

A Detailed Machinability Assessment of DC53 Steel for Die and Mold Industry through Wire Electric Discharge Machining

Sarmad Ali Khan [1], Mudassar Rehman [2], Muhammad Umar Farooq [1,3,*], Muhammad Asad Ali [1,*], Rakhshanda Naveed [1], Catalin I. Pruncu [4,5,*] and Waheed Ahmad [1]

[1] Department of Industrial and Manufacturing Engineering, University of Engineering and Technology Lahore, Lahore 54890, Pakistan; drsarmad@uet.edu.pk (S.A.K.); rakhshanda@uet.edu.pk (R.N.); 2012msime15@student.uet.edu.pk (W.A.)
[2] Department of Industrial Engineering, School of Mechanical Engineering, Northwestern Polytechnical University, Xi'an 710072, China; mudassar@mail.nwpu.edu.cn
[3] Department of Industrial and Systems Engineering, Korea Advanced Institute of Science and Technology, Daejeon 34141, Korea
[4] Department of Mechanical Engineering, Imperial College London, Exhibition Rd., London SW7 2AZ, UK
[5] Design, Manufacturing & Engineering Management, University of Strathclyde, Glasgow G1 1XJ, Scotland, UK
* Correspondence: umarmuf0@gmail.com (M.U.F.); asad.ali@uet.edu.pk (M.A.A.); c.pruncu@imperial.ac.uk or catalin.pruncu@strath.ac.uk (C.I.P.)

Abstract: Recently, DC53 die steel was introduced to the die and mold industry because of its excellent characteristics i.e., very good machinability and better engineering properties. DC53 demonstrates a strong capability to retain a near-net shape profile of the die, which is a very challenging process with materials. To produce complex and accurate die features, the use of the wire electric discharge machining (WEDM) process takes the lead in the manufacturing industry. However, the challenge is to understand the physical science of the process to improve surface features and service properties. In this study, a detailed yet systematic evaluation of process parameters investigation is made on the influence of a wire feed, pulse on duration, open voltage, and servo voltage on the productivity (material removal rate) and material quality (surface roughness, recast layer thickness, kerf width) against the requirements of mechanical-tooling industry. Based on parametric exploration, wire feed was found the most influential parameter on kerf width: KW (45.64%), pulse on time on surface roughness: SR (84.83%), open voltage on material removal rate: MRR (49.07%) and recast layer thickness: RLT (52.06%). Also, the optimized process parameters resulted in 1.710 μm SR, 10.367 mm^3/min MRR, 0.327 mm KW, and 10.443 μm RLT. Moreover, the evolution of surface features and process complexities are thoroughly discussed based on the involved physical science. The recast layer, often considered as a process limitation, was explored with the aim of minimizing the layers' depth, as well as the recast layer and heat-affected zone. The research provides regression models based on thorough investigation to support machinists for achieving required features.

Keywords: WEDM; DC53 steel; recast layer thickness; material removal rate; kerf

Citation: Khan, S.A.; Rehman, M.; Farooq, M.U.; Ali, M.A.; Naveed, R.; Pruncu, C.I.; Ahmqd, W. A Detailed Machinability Assessment of DC53 Steel for Die and Mould Industry through Wire Electric Discharge Machining. *Metals* **2021**, *11*, 816. https://doi.org/10.3390/met11050816

Academic Editor: George A. Pantazopoulos

Received: 7 April 2021
Accepted: 14 May 2021
Published: 17 May 2021

1. Introduction

Die-making industries employ a wide variety of engineering materials, such as variants of steel, for the fabrication of tools, dies, and molds based on their considerable application performance and increasing demand. Conventional steels involving D2 and D3 steel have been engaged for over a decade in the manufacturing of dies and molds. Among these steel families, DC53 steel is considered as an advancement over D2 and D3 steel in terms of its high hardness (64 HRC), better toughness, improved fatigue strength and wear resistance. Various engineering applications of DC53 steel involve the

manufacturing of different rolling, forging, injection molding, extrusion, and stamping dies along with molds, cutting tools, along with a wide variety of high speed and wear resistant parts [1].

The processing of such materials also becomes challenging as a result of their improved properties. Therefore, advanced machining setups are employed to fulfil the requirements. These involve electrochemical machining, electric discharge machining, plasma arc cutting, ultrasonic machining and abrasive water jet machining. These setups are considered an improvement in machining hard materials and generating a variety of machining profiles. Processing of hard materials such as titanium alloys and various other hardened steel grades—for instance, DC53 steel—may be difficult in a conventional machining scenario because of their excessive tool wear during machining. Therefore, non-conventional machining processes may be employed to serve the same purpose with little/no tool wear. Wire electric discharge machining (WEDM) is one of the non-traditional machining processes in which spark-based discharge energy is produced among two electrodes (wire electrode and workpiece) and responsible for material erosion during machining with no mechanical stresses generated unlike traditional machining processes [2].

WEDM is employed to process D2, D3 and different tool and die steel materials. Several investigations are made on the performance attributes like kerf width, material removal rate, and surface morphology, including roughness and microstructural examination involving recast layer [3–5]. The aspects of DC53 steel machining have not been thoroughly explored, therefore, are mainly investigated herein. Thiagarajan et al. [6] reported the combined influence of machining variables like pulse on duration (P_{on}), pulse off time (P_{off}), wire feed (WF) and wire tension (WT) at the MRR and SR in electric discharge machining of AISI D3 steel. A detailed study as multi-objective optimization was made by Manajaiah et al. [7] for AISI D2 steel in WEDM and inferred that the MRR, SR and recast layer thickness (RLT) are found in direct proportion with P_{on}. Ikram et al. [8] carried an insight investigation in WEDM of AISI D2 steel. The study reports that P_{on} is influenced more on SR (52.14%), MRR (49.62%), and KW (47.06%). In the study, results proved that P_{on} is two times more significant for SR compared to open voltage (OV), the combined influence of (WT, P_{on} and OV) found significant for KW, and the combination of servo voltage (SV), OV and P_{on} found significant for MRR respectively.

The experimental investigation performed by Vaghela et al. [9] for AISI D3 steel in WEDM inferred that the set of process variables peak current, P_{on} and P_{off} to maximize MRR, minimize KW and SR, respectively. Zhang et al. [10] performed mathematical modelling using back-propagation neural-network integrated with genetic algorithm and response surface methodology (RSM) to obtain optimal values of MRR and SR in WEDM of SKD11(D2 steel). Rupajati et al. [11] determined the machining performance regarding SR and recast layer thickness (RLT) for AISI H13 tool steel in electric discharge machining using Taguchi methodology along with the fuzzy-logic technique.

Significant improvements were obtained in RLT (22.04% reduction) and SR (13.15% reduction) from design of experiments results. It was also inferred that the significant variables for SR and RLT included P_{on} (40.08%) and O_V (30.38%), respectively. Hasriadi et al. [12] machined two different tool steel grades in WEDM for the assessment of surface morphology in terms of SR, RLT, and density of microcracks and resulted in the previously stated response variables forming a direct linear relation with both P_{on} and the arc on duration. Castillo et al. [13] explored the parametric effects on AISI 304 stainless steel.

Saini et al. [14] achieved multi-objective optimization in WEDM of 16MnCr5 alloy steel. Obwald et al. [15] conducted an analysis of different pulses types generated in high-speed WEDM. A detailed study was made by Solomon et al. [16] to comprehend the effect of variation in process variables for obtaining optimized parameters in WEDM of the steel family. Multi-objective optimization performed by Shivade and Shinde [17] in WEDM of AISI D3 steel resulted that gap current, and MRR varied directly with P_{on} and peak current, and inversely with the machining time (tm). Azam et al. [18] optimized cutting

speed (C.S) by the variation in P_{on}, P_{off}, and pulse frequency in WEDM of HSLA steel. The machined surface characterization was conducted by Dhobe et al. [19] in the electric discharge of AISI D2 steel. It was reported that RLT is found directly proportional with both SR and fatigue life. Based upon scanning electron microscopy (SEM) and X-ray diffraction results, it was reported that triple tempering (a heat treatment process) is better than single tempering as it improves the machined surface quality by reducing RLT and SR. Khanna and Singh [20] performed a comparative study in WEDM of cryogenic-treated and normal D3 tool steel for the cutting rate, MRR and SR. It was reported that the cryogenic treatment significantly influenced both the MRR (decreased 5.6%) and SR (surface finish increased 10.6%) compared to untreated D3 steel. Sharma et al. [21] endorsed similar findings on AISI D2 steel.

Ramaswamy et al. [22] predicted an optimal setting of machining parameters while performing optimization using a desirability function approach. Payla et al. [23] inferred that P_{on} directly influenced the MRR and power consumption during electric discharge machining of EN-31 die steel. It was also concluded that the MRR is reduced with an increase in SV because the energy density decreased as the spark gap expanded. Chen et al. [24] found that discharge capacitance has a direct and significant influence on MRR and the machining gap in microreciprocated WEDM of SKD11 (D2 steel). Singh et al. [25] supported the phenomenon for EN-31 tool steel. Abdulkareem et al. [26] worked to enhance the SR because of more adhesion of the debris particles and surface irregularities on the processed surface. Mouralova et al. [27] concluded that the frequency of discharge occurrence of the recast layer is highly influenced by cutting speed. Negrete [28] made a similar finding on AISI 01 tool steel. Kanlayasiri and Boonmung [1] investigated the influence of P_{on}, P_{off}, peak current and WT on SR in WEDM of DC53 steel. Nawaz et al. [29] used molybdenum to machine steel with the aim of achieving higher material removal rate and lesser surface roughness. The study quantified the influence of process in enhancing the pulse discharge energy because of the deeper craters produced on the machined surface. Similarly, Rehman et al. [30] evaluated gamma wire and resulted the significant influence of P_{on} for C.S (80.21%), KW (48.25%), and MRR (45.21%) during WEDM of DC53 steel.

The literature review reveals that a significant amount of work has already been done on various tools and die steels, especially D2, and D3 steel, to improve machining accuracy and productivity in wire electric discharge machining. However, we have noted a lack of systematic evaluation for the main parameters affecting the output responses in the WEDM of DC53 steel (having superior mechanical properties and machining performance over D2 and D3 steel), which was the key objective of this research. Moreover, the supremacy of zinc-coated brass wire (as recommended by literature) is not thoroughly studied, which may provide superior results as compared to previous established methodologies. To resolve this problem and further improve the state of the art, the following issue are discussed in this research:

- Investigating the influence of machining parameters on recast layer thickness (process limitation), surface roughness and kerf width (quality), and material removal rate (productivity).
- Optimizing input parameters such as wire feed (WF), pulse on duration (P_{on}), open voltage (OV), and servo voltage (SV) controlling process productivity and work quality of DC53 die steel processes with zinc-coated brass wire.
- Exploring the statistical significance of machining process science on physical changes on the material surface.
- Examining microstructural surface evolution using optical microscopy and scanning electron microscopy.

The results gathered in this work are of paramount importance for the forging industry (i.e., metal forming, flow forming, spinning) in order to create tools with higher integrity and superior surface characteristics.

2. Materials and Methods

DC53 steel has numerous applications in die- and mold-making industries and is the workpiece material for investigation. DC53 is a high chromium steel with high strength, good toughness, wear-resistance and excellent machinability over that of D2 and D3 steel. The composition details and other characteristics of DC53 are shown in Table 1. A DC53 steel flat bar was used with density of 7.85×10^3 kg⁄m^3. Experimental trials were performed in deionized water dielectric medium using zinc-coated brass wire of 0.25-mm diameter as an electrode on a CNC wire EDM setup (G43S CHMER, KNB Technologies Sdn Bhd, Malaysia). The wire electrode is recommended for fast-roughing and fine-trimming with low SR features providing less frequent breakage. Wire breakage is limiting phenomena that minimizes the productivity and upsurges the tooling cost. A detailed demonstration to illustrate the machining setup and 3D CAD view of the machined specimen accompanied by its dimensions are presented in Figure 1.

The effects of four machining variables, namely wire feed (WF), pulse on duration (P_{on}), open voltage (OV), and servo voltage (SV) have been carefully analyzed on the kerf width (KW), material removal rate (MRR), surface roughness (SR), and recast layer thickness (RLT). The choice of the said input parameters was made based on a comprehensive literature survey [1,15–17,19–25]. Additionally, preliminary experimentation (six trial experiments) was also performed before the mature experimentation to express the process parameter levels. In addition, the dielectric resistivity was carefully monitored and maintained at same level throughout the entire experimentation phase. Variables, in addition to the machining variables, were considered as the fixed factors. The particulars relating to the input variables and their ranges along with constant factors are reported in Table 2.

Table 1. Key features of DC53 steel.

DC53 Chemical Specifications		DC53 Characteristics [29–31]		
Element	**Wt (%)**	**Name**	**Unit**	**Value**
Carbon (C)	1.10	Modulus of elasticity	GPa	150
Chromium (Cr)	8.50	Modulus of rigidity	GPa	58.5
Molybdenum (Mo)	2.00	Rockwell hardness	HRC	64
Silicon (Si)	0.90	Poisson's ratio	-	0.28
Vanadium (V)	0.30	Thermal conductivity (at room temperature)	W/m-K	23.86
Manganese (Mn)	0.35	Coefficient of thermal expansion	1/°C	13×10^{-6}
Phosphorous (P)	0.03	Density	kg/m^3	7.85×10^3
Sulphur (S)	0.03	-	-	-
Iron (Fe)	BAL	-	-	-

The use of full factorial design as an experimental process involves the consumption of time and cost [32] compared to the Taguchi experimental design. The Taguchi methodology is considered useful because of its precise and robust analysis by a reduction in experimental runs [30]. Consequently, Taguchi's fractional factorial design orthogonal array (OA) has been used for performing the experimentation. In total, 18 experiments under mature experimentation were successfully completed using L_{18} OA and were followed by the measurement of the established output responses.

Table 2. Input machining variables levels along with response measures.

Process Variables	Symbol	Unit	Level			Output Responses	Symbol	Unit	Constant Parameters	Unit	Value
			1	2	3						
Wire feed	WF	mm/s	5	8		Kerf width	KW	µm	Pulse off-duration	µs	25
Pulse on-duration	P_{on}	µs	4	5	6	Surface roughness	SR	µm	Resistivity of dielectric	kg-Ω-cm	50–70
Open voltage	OV	volt	80	90	100	Material removal rate	MRR	mm^3/min	Wire tension	gms-f	1390
Servo voltage	SV	volt	40	50	60	Recast layer thickness	RLT	µm	Arc on time	µs	2

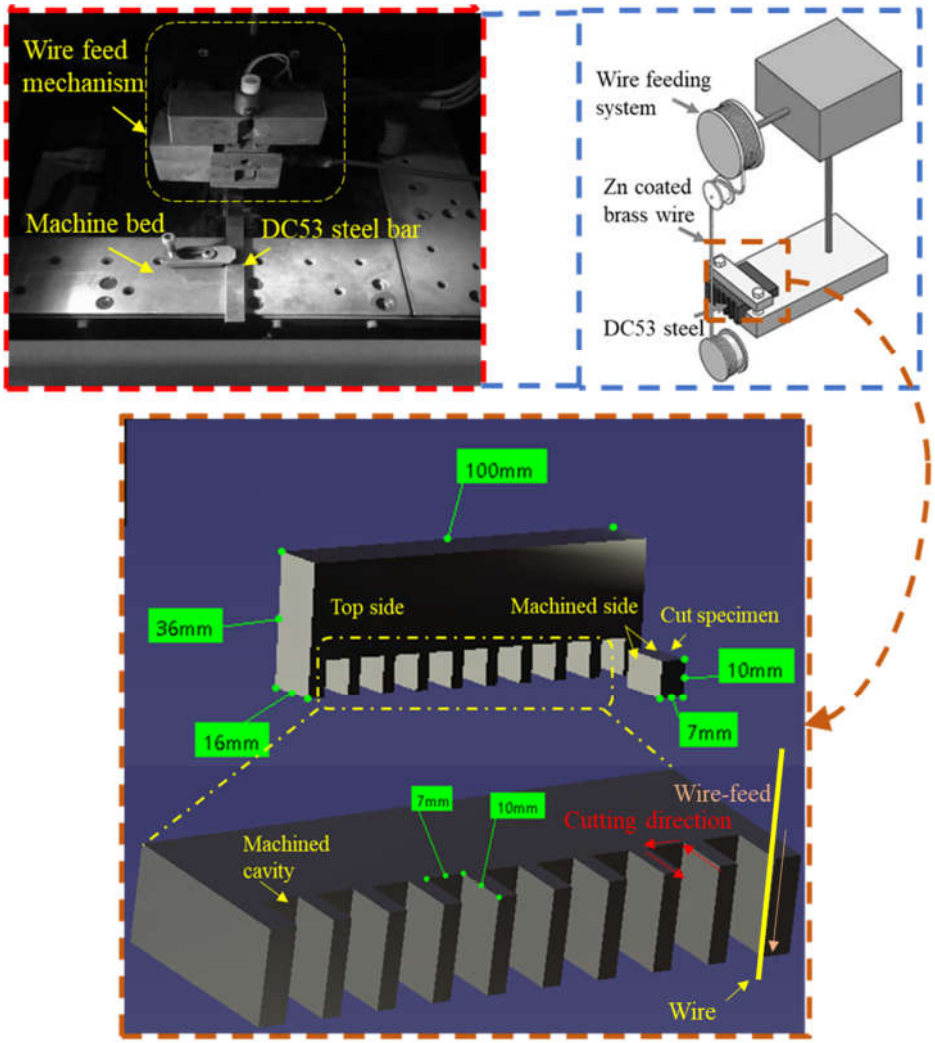

Figure 1. Illustration of experimental setup along with the workpiece.

Kerf-width is the measurement of extra material removed from the processed surface of the workpiece during machining. KW was examined by measuring the cutting slot distance using a calibrated video probe of a coordinate-measuring-machine (CMM) (CE-450DV, Chien Wei Precise Technology Co., Ltd., Fengshan District, Taiwan), as illustrated in Figure 2. MRR calculation methodology is reported in equation (1):

$$MRR = \left[\frac{W_b - W_a}{t_m * \rho_w}\right] \quad (1)$$

Where W_b and W_a denoted the weights of the workpiece before and after processing; t_m symbolized the machining time for each machining experiment, and ρ_w showed the workpiece density, respectively. The surface texture meter (Surtronic S128, Taylor Hobson

Leicester, United Kingdom) measured the surface roughness SR of the machined surface. The SR measurements were performed at three different points on the machined work surface by calibrating at an evaluation length of 4 mm and a cut-off length of 0.8 mm. The averages of measurements were used for analytical purposes. A scanning electron microscope (Vega 3-TESCAN, TESCAN, Brno, Czechia) was employed for microstructural examination of machined surface of the workpiece and recast layer thickness was measured by using optical microscope (Olympus MM6C-PS2, Olympus Corporation, Tokyo, Japan).

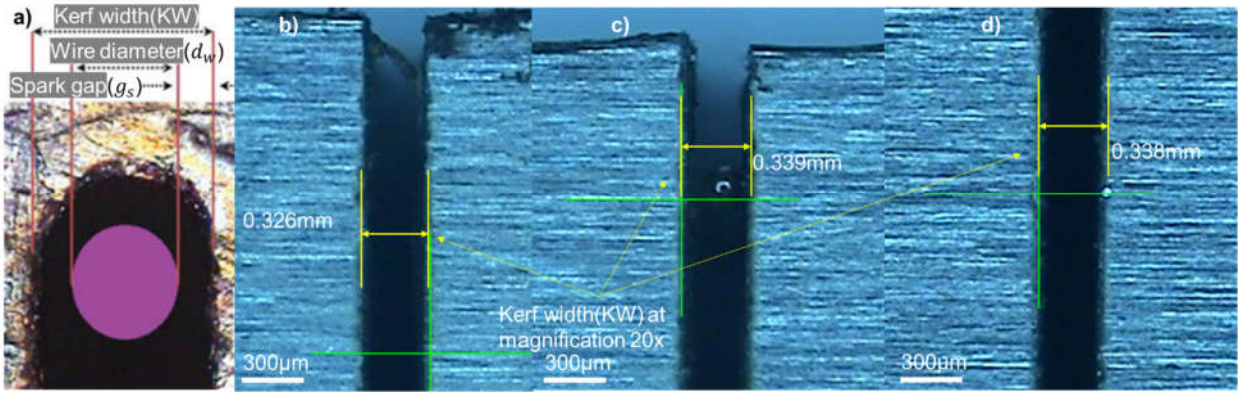

Figure 2. Schematic and physical representation of (**a**) kerf width along with physical evidence of its measurement using CMM, (**b**) For Exp. 1 (WF 5 mm/s, P_{on} 4 µs, OV 80 volt, SV 40 volt), (**c**) For Exp. 10 (WF 8 mm/s, P_{on} 4 µs, OV 80 volt, SV 60 volt), and (**d**) Exp. 18 (WF 8 mm/s, P_{on} 6 µs, OV 100 volt, SV 50 volt).

To carry out the microscopic examination, samples were prepared by mounting, etching, grinding and polishing. SEM-based morphological analysis was used to explain the process science and physical phenomenon. The statistical analysis was completed by using Minitab 19 software (Minitab, LLC, State College, Pennsylvania, USA). Confirmatory experimentation was performed based on parametric settings for the validation of research results.

3. Results and Discussion

The experimentation on the DC53 steel work part was successfully performed according to Taguchi L_{18} to examine and investigate the behaviour of input process variables for output responses. The results of the examination are more profoundly observed and analysed using statistical analysis techniques, optical microscopy and the scanning electron microscopy. These analyses are conducted to enlighten the machining effects along with process physics involved on the microstructure of machined surface. The design of experiments (DOE) results revealed that minimum kerf width (KW) of 0.318 mm, least (average) surface roughness (SR) of 1.69 µm, higher material removal rate (MRR) of 17.82 mm^3/min, and a least average recast layer thickness (RLT) of 9.63 µm were obtained. The obtained MRR results have shown maximum values as pulse on duration (P_{on}) was increased. In addition to this, KW, SR, and RLT values were also decreased by reducing P_{on} because it influenced directly on the number of sparks produced resulting in adequate melting of the workpiece during machining. The facts explanation pertaining to the analysis are stated in the upcoming segments of discussion in variance and trend analyses.

3.1. Parametric Significance Analysis

Variance analysis is considered a decisive tool to determine each process parameter's influence for a certain output response [8,30,33,34]. The insights of this analysis have been reported in Table 3, containing the *p*-value and percent contribution (PCR). The *p*-value

describes the significance in such a way that the process parameter with lower (<0.05) value is considered highly influential for a specific output response compared to other control variables [35]. The is because variables with a p-value ≤ 5% in statistical output data, indicating a 95% confidence interval, were regarded as significant with respect to other input parameters [33]. Percentage contribution is another tool to determine the more detailed control of the machining parameters on responses. In this study, PCR was estimated to evaluate and prioritize their significance in accordance with output responses as described by formula reported in Equation (2).

$$\text{Percentage contribution (PCR)} = \left[\frac{\text{Adj SS}}{\text{Total SS}} \times 100\right]\% \quad (2)$$

where Adj SS = Adjusted sum of squares, and Total SS = Total sum of squares are used from analysis of variance to calculate the contribution. The detailed results of variance analysis from Table 3 inferred that WF (45.648%), P_{on} (41.56%), and SV (3.77%) are the significant factors for KW. However, the detailed influential variables for SR include P_{on} (84.83%), WF (8.32%), OV (2.10%), and SV (1.15%). Open voltage, pulse on duration, and wire feed with percentage-contribution of 49.07%, 32.81%, and 10.51%, respectively, influenced on material removal. Continually, the significant variables for recast layer thickness involved OV (52.06%) and P_{on} (40%). Thorough analysis of the statistical data reported in Table 3 resulted in the finding that the pulse on duration: P_{on} was the common and most influential input parameter for all defined output responses in this study.

Table 3. Summary of analysis of variance.

Sr No.	Output Responses	*p* Value Variables				Percentage Contribution (PCR)				R-Sq (%)	R-Sq (Adj) (%)
		WF	P_{on}	OV	SV	WF	P_{on}	OV	SV		
1	Kerf width (KW)	**<0.001**	**<0.001**	0.08	**0.02**	45.64	41.56	1.95	3.77	92.95%	90.78%
2	Surface roughness (SR)	**<0.001**	**<0.001**	**0.016**	0.06	8.32	84.83	2.10	1.15	96.42%	95.31%
3	Material removal rate (MRR)	**0.001**	**<0.001**	**<0.001**	0.41	10.51	32.81	49.07	0.39	92.80%	90.58%
4	Recast layer thickness (RLT)	0.593	**<0.001**	**<0.001**	0.56	0.17	40.00	52.06	0.20	92.45%	90.13%

3.2. Process-Parametric Effect Analysis

The parametric-effect analysis was done to study the behaviour of process variables through graphical trends of output responses and the results based on statistical analysis. The analysis is shown in Figures 3–7.

3.2.1. Effects of the Wire Feed

The main effects result for WF, presented in Figure 3, has inferred that kerf width and surface roughness were decreased by increasing WF. The key reason behind this reduction is the rapid transport of wire, which resulted in less workpiece–wire electrode interaction, and produced a small heat-affected zone (HAZ). Moreover, it resulted in minor thermal damages, therefore, less molten material/debris was redeposited on the workpiece surface (will be revealed in Section 3.4). The machining efficiency of the wire electrode in WEDM was increased by increasing the WF. The effect was experienced irrespective of considering wire consumption because of a larger amount of the material removed in a shorter machining cycle was due to a rapid traverse of wire. Therefore, the material removal rate (MRR) increased with an increasing level of WF. Similar results on the wire feed were reported by Mussada et al. [36] and Negrete and Carmita [28]. It was confirmed that the increase in the WF assisted in the stable spark discharges produced and thus resulted in more melting and a redeposit of work material.

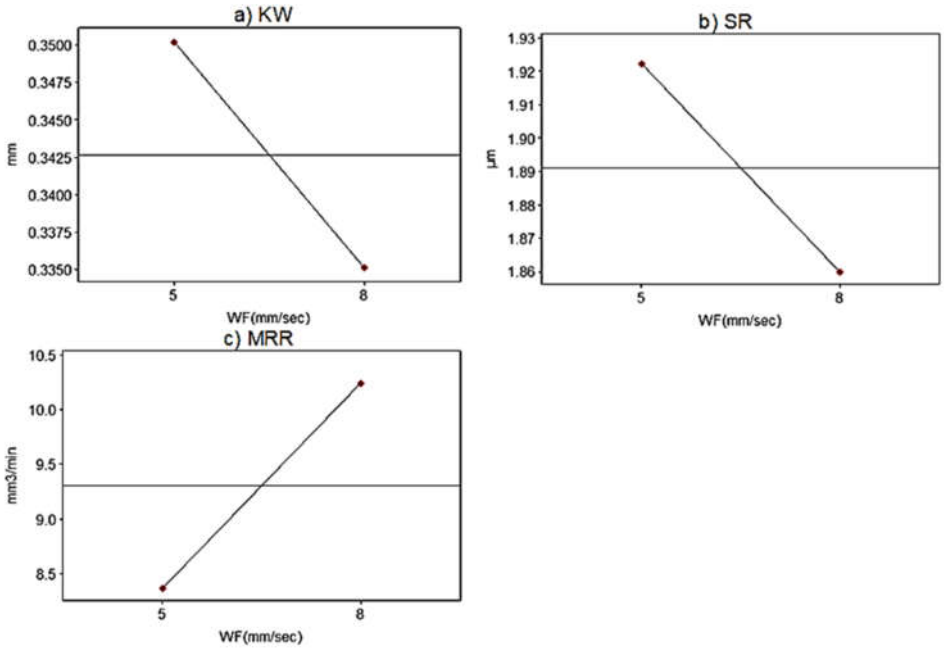

Figure 3. Parametric effects of wire feed (WF) for (**a**) kerf width (KW), (**b**) surface roughness (SR), and (**c**) material removal rate (MRR).

Kerf-width is defined as the measurement of excessive material removed during machining and its measurement demonstration is indicated in Figure 2. The analysis of means is shown as main effect plots in Figure 3a. It indicated an inverse relationship of WF with KW. The decreasing trend is observed for KW from 0.350 to 0.335 mm by increasing WF level from 5 to 8 mm/s. The rationale behind this effect lies in the minimal spark gap produced because of enhanced WF. The continual incoming fresh wire assisted in the minimizing the workpiece–wire electrode interaction time, and thus reduced the removal of excessive material from the work surface during machining.

However, the excessive increase in the WF produces irregularities on the machined surface, as reported by Somashekhar et al. [37]. The intensity of the current is enhanced because of consistent incoming fresh wire. This is because of the availability of increasingly present fresh ions and interacting surface. Furthermore, the wire breakage frequency may also be reduced because of adequate increase in WF. The decrease in KW happened at low P_{on} values. Hence, the kerf width is decreased by increasing the wire feed. Based on variance analysis from Table 3, the wire feed was also found to be top significant factor for kerf width (45.64%) compared to other process variables.

Surface roughness is the measurement of surface asperities on the machined surface [38]. The graphical trends of WF for SR from Figure 3b have resulted that the surface roughness was declined from 1.92 to 1.86 µm because of increased levels of wire feed. This is because of less contact duration between the wire electrode and the workpiece. Therefore, a greater amount of debris is flushed away by the dielectric and less discrepancies occurred on the machined surface thus resulted in small SR. Similar findings were identified by Tilekar et al. [39] and it was also inferred that the incoming fresh wire in the machining zone assisted in reducing the heat energy (function of heat transfer and plasma generation) because of instability of discharges resulting from higher wire feed which produced less irregularities on the machined surface. In addition, increased wire feed decreases the spark stability time due to the speedy motion of the wire and increases the tooling cost (similar science is discussed by Farooq et al. [40]). ANOVA observations also indicated that WF was identified as the influential factor for SR (8.20%).

The material removal rate is the measurement of amount of material-removed in a particular machining time [38]. Higher MRR is usually desired to enhance the overall machining productivity of the machine and the process. The results data have indicated that the MRR increased from 8.5 to ~10.3 mm^3/min by increasing the WF values (Figure 3c). The reason is the improved stability of thermal energy produced in the cutting zone with the help of constantly moving electrode wire. This has caused an increase in the sparks density in a shorter duration of machining cycle, which leads to enhance material melting and vaporization and thus resulted in more MRR. The comparison of the MRR trends was made with the existing literature and similar findings were obtained [37]. Wire feed was found to be significant variable for MRR (10.51%) as viewed from the variance analysis in Table 3.

3.2.2. Effects of Pulse-On Duration

The analysis of the parametric effects of pulse-on duration on the selected output responses is indicated in Figure 4. It is generally said that P_{on} plays its key role in improving the machining performance/machinability of WEDM. The statistical data results have elaborated that all the response measures namely KW, SR, MRR and RLT were linearly boosted up by increasing P_{on}. The reason is that by increasing this variable leads to increase in the discharge energy among two electrodes and creates a plasma energy channel among the workpiece and wire electrode gap. This plasma channel consists of pool of electrons and ions melted material because of the generation of an adequate heat-affected zone on the machined surface. Therefore, it usually plays an important role in influencing on the machining quality. Similar insights were reported by Rehman et al. [30] and coherent results were obtained in their experimental investigation.

The graphical trend of P_{on} for KW is similar as of WF for MRR. The parametric plots from Figure 4a have shown the direct effect of pulse-on duration (P_{on}) on KW, which means that kerf width is alleviated by varying the duration of pulses. This was because the number of sparks was amplified by increasing the time interval, resulting in the enhancement of the sparks energy and thus, a larger heat-affected zone was produced. The kerf width was increased by increasing the pulse duration. However, the analysis of trends also inferred that a small increase in KW was obtained when the pulse on duration was increased to one upper level from 4 to 5 μs, whereas a sudden increase in the KW was observed as P_{on} was promoted from 5 to 6 μs. However, 5 μs is a threshold level of the pulse on duration, after which relatively more thermal energy is produced to melt the extra material from the sides of the workpiece because of consistently increasing sparks erosion. The variance analysis findings have also proved the most influential of P_{on} (41.56%) for KW.

The trend analysis of P_{on} is shown in Figure 4b,c for surface roughness (SR) and material removal rate (MRR), respectively. The melt material is highly depended on increased number of discharges and the discharge energy generates a large pool of electrons and ions. Thus, with the increase in the amount of material removed and surface asperities on the machined surface of the workpiece also increase. Pulse duration was found as the most remarkable parameter for SR (84.83%) and also influential variable for MRR (32.81%).

The white layer is produced during machining when the leftover melt material re-solidifies on the machined surface of the workpiece [41]. Therefore, the recast layer thickness plays a vital role in evaluating the surface integrity of the machined specimen. The number of leftover debris and unflushed material on the surface has increased linearly with the increase of spark on duration. The reason is thermally affected region due to enhanced thermal energy and stability of sparks because of more spark's duration. Therefore, the number of unflushed particles were increased as the P_{on} is increased from 4 to 6 μs, resulting in a greater recast layer thickness, as shown in Figure 4d. A microscopic overview of the recast layer formation is shown in Figure 5. The craters produced are

shallow and wider whereas the density of microcracks formation is also increased by increasing the P_{on}.

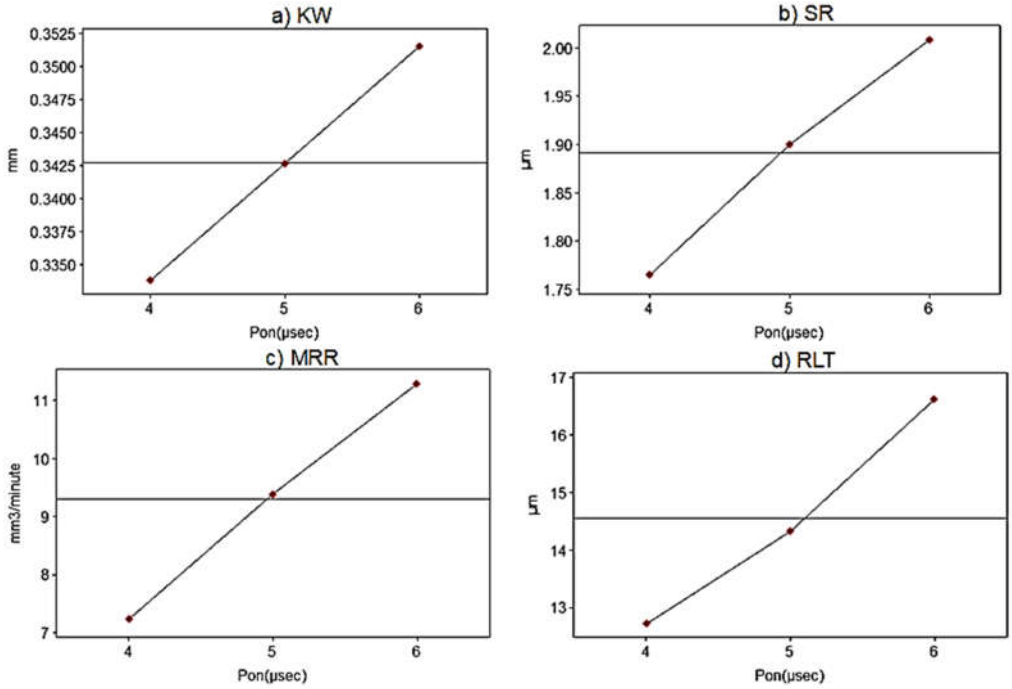

Figure 4. Parametric effects of pulse on duration (P_{on}) for (**a**) kerf width (KW), (**b**) surface roughness (SR), (**c**) material removal rate (MRR), and (**d**) recast layer thickness (RLT).

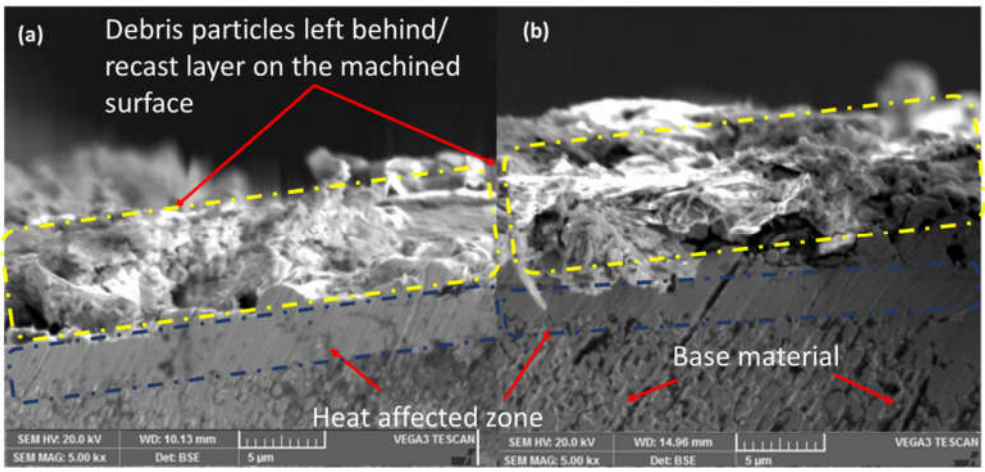

Figure 5. Representation of the recast layer formed on the machined work surface at random experimental settings (**a**) P_{on} 4 µsec (**b**) P_{on} 5 µsec.

3.2.3. Effects of Open Voltage

The role of the open voltage is to perform a thermal breakdown to generate plasma channel [33]. SR was enhanced greatly by increasing OV as can be seen in Figure 6. SR possessed a direct relationship with OV similar to RLT. The thorough analysis of observations indicated that the increase in OV resulted in increasing SR, and RLT. The key reason involves discharge energy phenomenon because of thermal breakdown during machining.

The plasma channel width is increased because of the enhanced open voltage levels resulting in a larger thermal affected zone. The surface irregularities were increased at

higher values of OV as shown in Figure 6a. The surface asperities are enhanced because of increased discharge energy. This enlarged the width of the plasma channel, creating deeper craters. The volume of the material removed was decreased by increasing the OV from 80 to 100 V because of the instability of discharge energy (Figure 6b). The phenomenon involves inadequate melt generation due to a small amount of thermal energy and poor flushing conditions, resulting in the insufficient removal of melt. OV was found to have significant influence (49.07%) in controlling MRR.

The thickness of the recast layer increased linearly by enhancing the OV, as presented in Figure 6c. In this case, from OV from 80 to 100 V, a linearly increasing trend of RLT is observed similar to SR was obtained due to plasma energy channel. It was produced because the material was melted and redeposited in the surface. Therefore, discharge energy was enhanced by increasing OV leaving more material behind on the work surface. The open voltage was found as foremost significant variable (52.06%) compared to other variables affecting the recast layer thickness.

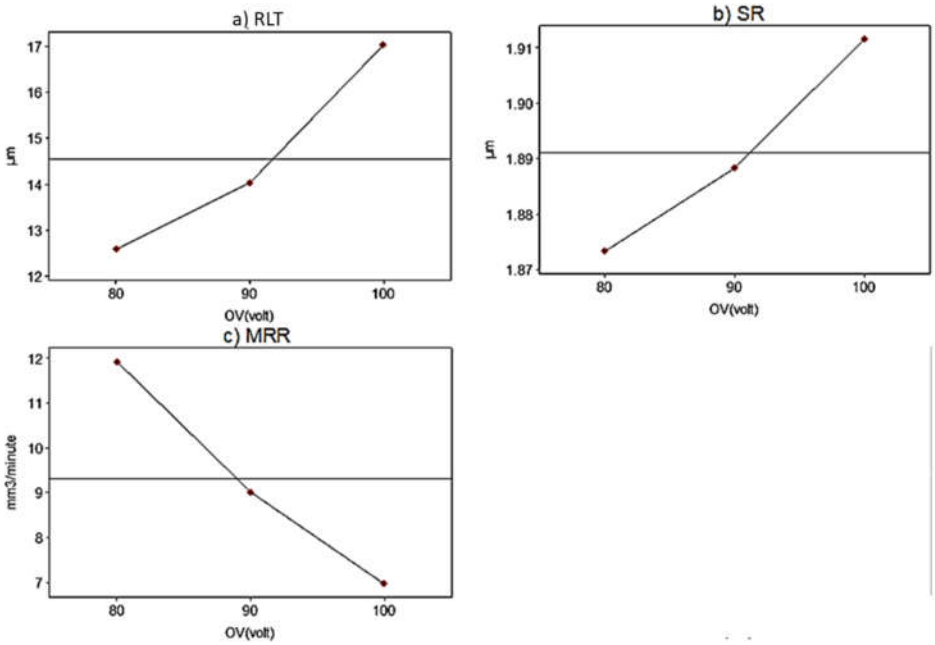

Figure 6. Parametric effects of open voltage (OV) for (**a**) recast layer thickness (RLT), (**b**) surface roughness (SR), (**c**) material removal rate (MRR).

3.2.4. Effects of Servo Voltage

Servo voltage is usually responsible for the transfer of heat flux on the dedicated workpiece surface through controlling the workpiece and wire electrode gap. All the output responses possessed quadratic behaviour by increasing the SV. A detailed discussion of SV provided herein, and trends are shown in Figure 7.

Kerf width was increased gradually by increasing the SV from 40 to 50 V. The rationale of the gradual increase in KW at the first two levels of SV is the relatively small amount of erosion of the material from both edges of the workpiece. However, a relatively greater increase in KW with increased servo voltage levels from 50 to 60 V is due to increased spark gap between the wire and workpiece electrodes, which resulted in a wider kerf. The phenomenon behind the increasing trend of KW was endorsed by Rehman et al. [30].

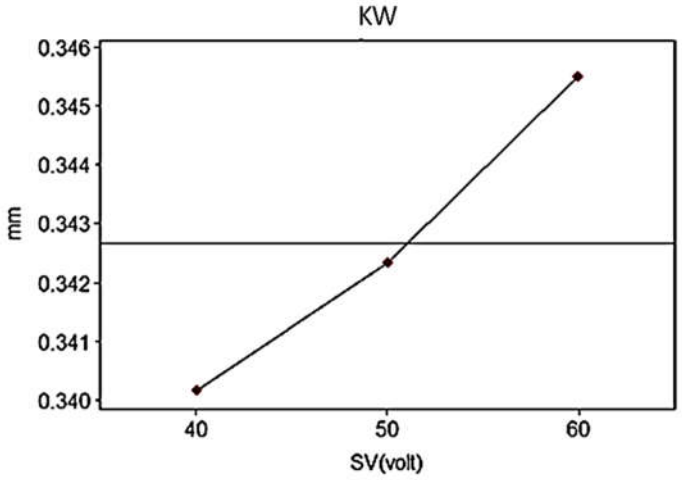

Figure 7. Parametric effects of servo voltage (SV) for kerf width (KW).

3.3. Mathematical Modelling and Parametric Optimization

To determine the predictability of responses (productivity and quality), the general regression model is developed through converting variable parameters to continuous predictive variables [42]. The general algebraic expression of model is given as following.

$$y = b_0 + b_1x_1 + b_2x_2 \ldots \ldots \ldots \ldots + b_kx_k \quad (3)$$

In the general model, y represents the value of the response while b_0 is the constant value and b_1, b_2, b_3, …, b_k represents the estimated variation in mean response for each unit change in the variable parameters. Experimental data was used to generate regression models using variable parameters as continuous predictors. The relationship of WEDM variable parameters on productivity quality measures using multiple regression analysis.

$$\text{RLT} = -14.03 - 0.070\,\text{WF} + 1.947\,\text{Pon} + 0.2222\,\text{OV} - 0.0139\,\text{SV} \quad (4)$$

$$\text{W} = 0.3007 - 0.005037\,\text{WF} + 0.00883\,\text{Pon} + 0.000192\,\text{OV} + 0.000267\,\text{SV} \quad (5)$$

$$\text{SR} = 1.3159 - 0.02074\,\text{WF} + 0.12167\,\text{Pon} + 0.001917\,\text{OV} - 0.001417\,\text{SV} \quad (6)$$

$$\text{MRR} = 18.53 + 0.624\,\text{WF} + 2.027\,\text{Pon} - 0.2478\,\text{OV} - 0.0223\,\text{SV} \quad (7)$$

Where "WF", "P_{on}", "OV" and "SV" are representing wire feed (mm/s), pulse on time (μs), open voltage (V), and servo voltage (V), respectively.

Utilizing the experimental data, Minitab 19 was used to develop multiple regression models associated with recast layer thickness, kerf width, surface roughness and material removal rate presented in Equations (4)–(7), respectively. The output values of the response measures were predicted after obtaining the optimal parameters for each response, and the optimization results were validated by performing confirmatory experiments. The results of the experimentation (three experiments) as a result of this optimization produced a very minute standard deviation from the design of experiments results.

Moreover, the desirability function was employed to optimize process settings, such as the minimum, which was better for recast layer thickness, kerf width, surface roughness, and the maximum, which was better for the material removal rate. The results of the experimentation provided a major process improvement. The optimized parameters obtained are "WF 8 mm/s", "P_{on} 4 μs", "OV 80 V" and "SV 56V". In Table 4, the close agreement is shown between the predicted values and experimental trials on the optimized process settings ensures the adequacy of empirical models.

Table 4. Measured responses on optimized process parameters.

Sr. No.	Process Parameters				Response Indicators			
	WF (mm/s)	P_{on} (µs)	OV (V)	SV (V)	SR (µm)	MRR (mm^3/min)	KW (mm)	RLT (µm)
1	8	4	80	56	1.709	10.307	0.327	10.093
2	8	4	80	56	1.703	10.299	0.326	10.256
3	8	4	80	56	1.719	10.496	0.330	10.980
	Avg. experimental value				1.710	10.367	0.327	10.443
	Standard deviation				0.006	0.091	0.001	0.385
	Predicted value				1.711	10.554	0.326	10.191
	Error %				0.64	1.77	0.31	2.47

3.4. Recast Layer Measurement and Microstructural Evaluation

The microscopic analysis is usually performed to analyse the physical phenomena on the surface morphology of the workpiece. The optical and scanning electron microscopy-based analyses are explored herein.

3.4.1. Optical-Based Microscopic Analysis

The detailed recast layer thickness analysis was carried out through optical microscope, (Figure 8A,B) to investigate the physics involved on the morphological alterations on the workpiece surface. The recast layer was measured at three distinct positions on the processed surface and average of the measurements was chosen for the analysis purpose.

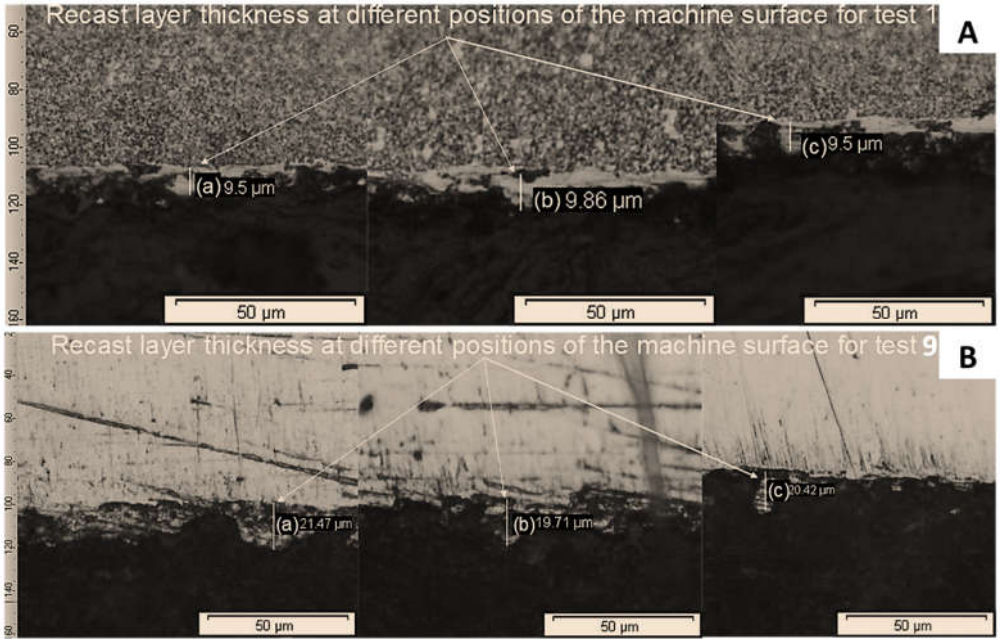

Figure 8. Optical microscopic examination (at three different points for one experiment) for recast layer measurement at different parametric settings for (**A**) WF 5 mm/s, Pon 4 µs, OV 80 V, and SV 40 V (**B**) WF 5 mm/s, Pon 6 µs, OV 100 V, and SV 40 V.

It can be extracted from Figure 8A,B that the significant thickness is deposited on the base metal layer. Its microstructure is different from the unaffected surface consisting of primary carbides. It was inferred that the maximum recast layer thickness of 19.52 µm was obtained at the minimum WF (5 mm/s), high level of P_{on} (6 µs), higher value of OV (100 V), and the minimum SV (40 V). Similarly, the higher control is responsible for the thermal breakdown to improve the sparks' stability and smaller control level means that the sparks energy is focused on the specific region where material melting and

redeposition occurred. Therefore, the recast layer thickness was increased at these parametric settings. Similarly, a minimum RLT was observed at WF 5 mm/s, P_{on} (4 µs), OV (80 V), and SV (40 V). The reason is that the debris redeposition is decreased as the sparks on duration is decreased because P_{on} is highly influential parameter for the recast layer thickness compared to other variables.

3.4.2. Scanning Electron Microscopic Analysis

The detailed investigation for the microstructure of the processed surface is demonstrated in Figure 9a,b. The evidence shows that microcracks appeared on the machined surface. Moreover, the properties of melt material redeposit on machined surface varied because of bonding and cracks generated in heat effected region. The recast layer properties are primarily different from the base metal because of heat treatment and quenching, as shown in Figure 9. The thermal energy generated between wire electrodes results in enlarged heat effected zone produced on the machined surface, providing opportunity to redeposit onto the machined layer.

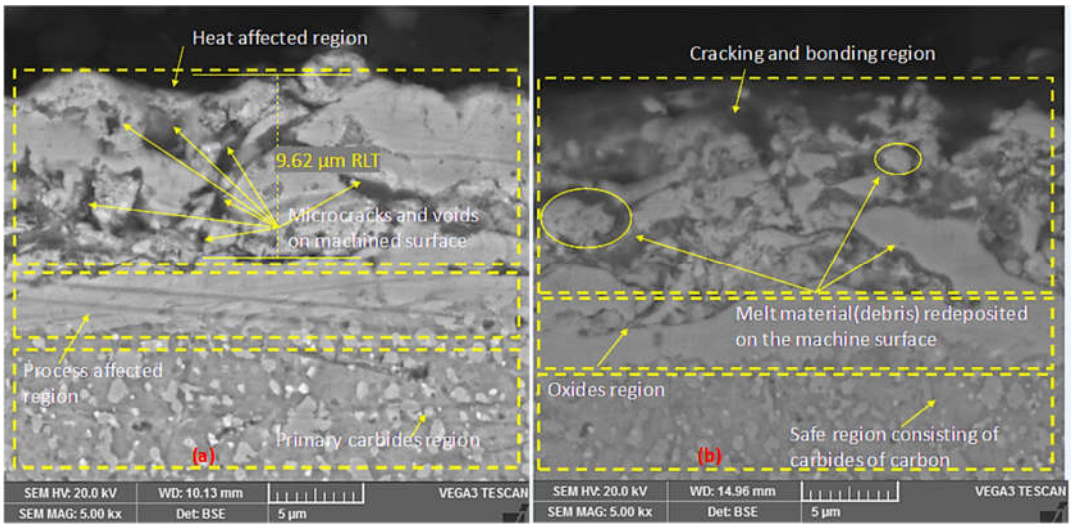

Figure 9. Scanning electron microscopy results of machined specimens (**a**) WF1, Pon1, OV2, SV2, (**b**) WF1, Pon3, OV1, and SV2.

It can be seen from Figure 9 that the craters of different sizes and shapes, microcracks and thermally redeposit melt material/debris were evident on machined surface. The density of crack formation and the size of the craters increased by increasing the sparks-on duration (the discharge energy is linearly dependent on it). Likewise, the process is influenced by process variables on the microstructural evaluation, as evident from Table 3. Similarly, pulse on duration influenced its maximum on controlling the craters size, density of cracks formation, and size of debris globules formed on the processed surface. The measured RLT on the machined surface was found 9.62 µm. The analysis of SEM images from Figure 9 inferred that an oxide layer formed just below the heat-affected layer. This process-affected region was generated because of large plasma channel width, resulting in more irregularities on the machined surface. The layer below the process affected zone was considered as the safe region, consisting of primary carbides of carbon.

3.5. Comparison with Previous Studies

The tabular comparison of current output results was also compared with the published literature for DC53 steel in WEDM and summary is reported in Table 5. The research findings were found almost in good agreement with the existing results which also validated the experimental work. In addition, machinability of DC53 steel with zinc-coated wire produced superior results in comparison to established practices [29,30].

Table 5. Comparison of the obtained results with the existing literature.

Output Response	Unit	Current Work	Previous Work on Steel	References
SR	μm	1.71	1.72, 1.89, 1.68	[1,29,30]
MRR	mm^3/min	10.367	5.443, 10.205	[29,30]
KW	mm	0.327 (at 0.25 mm wire Φ)	0.220, 0.287 (at 0.20 mm wire Φ)	[29,30]
RLT	μm	10.443	-	-

4. Conclusions

This work was dedicated to providing experimental insight into the machining of DC53 die steel, and considering the most important process variables, namely wire feed-WF, pulse on duration-P_{on}, open voltage-OV, and servo voltage-SV. The influence of these variables on kerf width-KW, surface roughness-SR, material removal rate-MRR, and recast layer thickness-RLT during wire electric discharge machining was studied. Through rigorous analysis based on physical phenomenon on surface morphology and material characteristics, the following conclusions are extracted:

- RLT was directly influenced by varying the P_{on} and it was observed that SEM examination revealed three surface regions; (i) thermally affected region consisting of debris particles of different sizes and shapes, cracks and craters, (ii) process-affected zone consisting of oxides, and (iii) safe region consisting of the primary carbides of carbon. Minimum average RLT of 9.63 μm was measured and observed after the examination of machined surface morphology.
- The variance analysis results inferred that P_{on} was found to be the most significant machining variable for all output responses with higher contribution percentages such as SR (84.83%), KW (41.56%), RLT (40.00%), and MRR (32.81%), respectively. High P_{on} results ina high plasma channel consisting the pool of electrons and ions melted material because of the generation of an adequate heat-affected zone on the machined surface.
- WF (45.64%), P_{on} (41.56%), and the SV (3.774%) are the significant factors for KW. However, the detailed influential variables for SR include P_{on} (84.83%), WF (8.320%), OV (2.10%), and SV (1.15%). The significant variables for recast layer thickness involved OV (52.06%) and P_{on} (40.00%). Open voltage, pulse on duration, and wire feed with percentage contributions of 49.07%, 32.81%, and 10.51%, respectively, are significant for MRR. The rapid transport of wire resulted in less workpiece–wire electrode interaction, and produced a smaller heat-affected zone because of minor thermal damages. Therefore, less molten material was redeposited on the workpiece surface.
- The experimental results reveal that WF influences prominently in reducing KW, SR, and RLT and increasing MRR. All response measures were directly increased by increasing P_{on} due to the amplified discharge energy of the sparks produced.
- The optimized parameters obtained are "WF 8 mm/s", "P_{on} 4 μs", "OV 80 V" and "SV 56 V" resulting 1.710 μm SR, 10.367 mm^3/min MRR, 0.327 mm KW, and 10.443 μm RLT. The regression models (showing less than a 3% error from the physical experimentation) are developed based on a thorough investigation to support the machinists for achieving the required features.

Future work that could further improve the quality of dies tools should be focused on experimental investigation using other control variables like flushing pressure, wire tension, and corner accuracy (both top and bottom) in WEDM of DC53 steel using different wire electrodes.

Author Contributions: Conceptualization, S.A.K. and W.A.; Data curation, W.A.; Formal analysis, R.N. and M.R.; Funding acquisition, M.U.F., M.A.A. and C.I.P.; Investigation, W.A., M.R. and R.N.;

Methodology, S.A.K. and M.R.; Resources, R.N.; Software, W.A. and M.R.; Supervision, S.A.K.; Validation, S.A.K., R.N. and C.I.P.; Visualization, M.U.F., M.A.A. and C.I.P.; Writing—original draft, M.U.F., M.R. and M.A.A.; Writing—review & editing, M.U.F., M.A.A., C.I.P. All authors have read and agreed to the published version of the manuscript.

Funding: This study did not receive any funding.

Institutional Review Board Statement: Not applicable.

Informed Consent Statement: Not applicable.

Data Availability Statement: The data is available as request from corresponding authors.

Conflicts of Interest: The authors declare no conflicts of interest.

Abbreviations

ANOVA	Analysis of variance
CMM	Coordinate measuring machine
DOE	Design of experiments
HAZ	Heat affected zone
KW	Kerf width (μm)
MRR	Material removal rate (mm^3/min)
OV	Open voltage (volt)
OA	Orthogonal array
ρ	Density (kg/m^3)
PCR	Percent contribution (%)
Pon	Pulse on duration (μs)
Poff	Pulse off time (μs)
RLT	Recast layer thickness (μm)
SR	Surface roughness (μm)
SV	Servo voltage (volt)
SEM	Scanning electron microscopy
WEDM	Wire electric discharge machining
WF	Wire feed (mm/s)
WT	Wire tension (gms-f)
W_b	Weight of the workpiece prior machining (g)
W_a	Weight of the workpiece prior after machining (g)

References

1. Kanlayasiri, K.; Boonmung, S. Effects of wire-EDM machining variables on surface roughness of newly developed DC 53 die steel: Design of experiments and regression model. *J. Mater. Process. Technol.* **2007**, *192*–193, 459–464, doi:10.1016/j.jmatprotec.2007.04.085.
2. Singh, V.; Bhandari, R.; Yadav, V.K. An experimental investigation on machining parameters of AISI D2 steel using WEDM. *Int. J. Adv. Manuf. Technol.* **2017**, *93*, 203–214, doi:10.1007/s00170-016-8681-6.
3. Durairaj, M.; Sudharsun, D.; Swamynathan, N. Analysis of process parameters in wire EDM with stainless steel using single objective Taguchi method and multi objective grey relational grade. *Procedia Eng.* **2013**, *64*, 868–877, doi:10.1016/j.proeng.2013.09.163.
4. Zhang, G.; Zhang, Z.; Guo, J.; Ming, W.; Li, M.; Huang, Y. Modeling and optimization of medium-speed WEDM process parameters for machining SKD11. *Mater. Manuf. Process.* **2013**, *28*, 1124–1132, doi:10.1080/10426914.2013.773024.
5. Lodhi, B.K.; Agarwal, S. Optimization of machining parameters in WEDM of AISI D3 steel using taguchi technique. *Procedia CIRP* **2014**, *14*, 194–199, doi:10.1016/j.procir.2014.03.080.
6. Thiagarajan, C.; Sararvanan, M.; Senthil, J. Performance Evaluation of Wire Electro Discharge Machining on D3-Tool Steel. *Int. J. Pure Appl. Math.* **2018**, *118*, 943–949.
7. Manjaiah, M.; Laubscher, R.F.; Kumar, A.; Basavarajappa, S. Parametric optimization of MRR and surface roughness in wire electro discharge machining (WEDM) of D2 steel using Taguchi-based utility approach. *Int. J. Mech. Mater. Eng.* **2016**, *11*, 7, doi:10.1186/s40712-016-0060-4.
8. Ikram, A.; Mufti, N.A.; Saleem, M.Q.; Khan, A.R. Parametric optimization for surface roughness, kerf and MRR in wire electrical discharge machining (WEDM) using Taguchi design of experiment. *J. Mech. Sci. Technol.* **2013**, *27*, 2133–2141, doi:10.1007/s12206-013-0526-8.

9. Vaghela, J.R.; Valaki, J.B.; Pandit, J.H. Parametric Optimization of Machining Parameters of AISI D3 Tool Steel Using Wire Cut Electric Discharge Machining—A Taguchi Based Approach. *Natl. Conf. Emerg. Res. Trends Eng*. **2016**. Available online: https://www.researchgate.net/publication/300262070 (accessed on 22 March 2021).
10. Zhang, G.; Zhang, Z.; Guo, J.; Ming, W.; Li, M.; Huang, Y.; Shao, X. The multi-objective optimization of medium-speed WEDM process parameters for machining SKD11 steel by the hybrid method of RSM and NSGA-II. *Int. J. Adv. Manuf.* **2014**, *70*, 2097–2109, doi:10.1007/s00170-013-5427-6.
11. Rupajati, P.; Soepangkat, B.O.P.; Pramujati, B.; Agustin, H.C.K. Optimization of Recast Layer Thickness and Surface Roughness in the Wire EDM Process of AISI H13 Tool Steel Using Taguchi and Fuzzy Logic. *Appl. Mech. Mater.* **2014**, *493*, 529–534, doi:10.4028/www.scientific.net/AMM.493.529.
12. Hasriadi, Soepangkat, B.O.P.; Subiyanto, H. The Effects of Pulse on Time and Arc on Time on Surface Quality in Wire-EDM of ASSAB XW-42 and ASSAB 8407 2M Tool Steels. *Appl. Mech. Mater.* **2016**, *836*, 173–178, doi:10.4028/www.scientific.net/AMM.836.173.
13. Hernández-Castillo, I.; Sánchez-López, O.; Lancho-Romero, G.A.; Castañeda-Roldán, C.H. An experimental study of surface roughness in electrical discharge machining of AISI 304 stainless steel. *Eng. Res.* **2018**, *38*, 90–96, doi:10.15446/ing.investig.v38n2.67711.
14. Saini, T.; Goyal, K.; Bhandari, D. Multi-response optimization of *WEDM* parameters on machining 16MnCr5 alloy steel using Taguchi technique. *Multiscale Multidiscip. Model. Exp. Des.* **2018**, doi:10.1007/s41939-018-0027-7.
15. Oßwald, K.; Lochmahr, I.; Schulze, H.P.; Kröning, O. Automated Analysis of Pulse Types in High Speed Wire EDM. *Procedia CIRP* **2018**, *68*, 796–801, doi:10.1016/j.procir.2017.12.157.
16. Solomon, R.S.; Sevvel, P.; Jaiganesh, V.; Satheesh, C. An Investigational Review on Influence of Performance Parameters during Wire Electrical Discharge Machining of Various Grades of Steels. *J. Adv. Res. Dyn. Cont. Sys.* **2017**, *9*, 101–109.
17. Shivade, A.S.; Shinde, V.D. Multi-objective optimization in WEDM of D3 tool steel using integrated approach of Taguchi method & Grey relational analysis. *J. Ind. Eng. Int.* **2014**, *10*, 149–162, doi:10.1007/s40092-014-0081-7.
18. Azam, M.; Jahanzaib, M.; Abbasi, J.A.; Wasim, A. Modeling of cutting speed (CS) for HSLA steel in wire electrical discharge machining (WEDM) using moly wire. *J. Chin. Inst. Engr.* **2016**, *39*, 802–808, doi:10.1080/02533839.2016.1191377.
19. Dhobe, M.M.; Chopde, I.K.; Gogte, C.L. Investigations on Surface Characteristics of Heat Treated Tool Steel after Wire Electro-Discharge Machining Investigations on Surface Characteristics of Heat Treated Tool Steel after Wire Electro-Discharge Machining. *Mater. Manuf. Process.* **2013**, *28*, 1143–1146, doi:10.1080/10426914.2013.822976.
20. Khanna, R.; Singh, H. Comparison of optimized settings for cryogenic-treated and normal D-3 steel on WEDM using grey relational theory. *Proc. Inst. Mech. Eng. Part L: J. Mater. Des. Appl.* **2016**, *230*, 219–232, doi:10.1177/1464420714565432.
21. Sharma, S.; Kumar Vates, U.; Bansal, A. Parametric optimization in wire EDM of D2 tool steel using Taguchi method. *Mater. Today Proc* **2020**, doi:10.1016/j.matpr.2020.02.802.
22. Ramaswamy, A.; Perumal, A.V.; Jagadeesan, J.; Nagarajan, H.V. Optimization of WEDM process parameters for D3 die steel using RSM. *Mater. Today Proc.* **2020**, *37*, 2063–2069, doi:10.1016/j.matpr.2020.07.50.
23. Payla, A.; Chopra, K.; Mussada, E.K. Investigations on power consumption in WEDM of EN31 steel for sustainable production. *Mater. Manuf. Process.* **2019**, *34*, 1855–doi:10.1080/10426914.2019.1683577.
24. Chen, X.; Wang, Z.; Wang, Y.; Chi, G. Investigation on MRR and Machining Gap of Micro Reciprocated Wire-EDM for SKD11. *Int. J. Precis. Eng. Manuf.* **2020**, *21*, 11–22, doi:10.1007/s12541-019-00233-7.
25. Singh, S.; Maheshwari, S.; Pandey, P.C. Some investigations into the electric discharge machining of hardened tool steel using different electrode materials. *J. Mater. Process. Technol.* **2004**, *149*, 272–277, doi:10.1016/j.jmatprotec.2003.11.046.
26. Abdulkareem, S.; Khan, A.A.; Zain, Z.M. Experimental investigation of machining parameters on surface roughness in dry and wet wire-electrical discharge machining. *Adv. Mater. Res.* **2011**, *264–265*, 831–836, doi:10.4028/www.scientific.net/AMR.264-265.83.
27. Mouralova, K.; Benes, L.; Bednar, J.; Zahradnicek, R.; Prokes, T.; Matousek, R.; Hrabec, P.; Fiserova, Z.; Otoupalik, J. Using a DoE for a comprehensive analysis of the surface quality and cutting speed in WED-machined hadfield steel. *J. Mech. Sci. Technol.* **2019**, *33*, 2371–2386, doi:10.1007/s12206-019-0437-4.
28. Camposeco-Negrete, C. Prediction and optimization of machining time and surface roughness of AISI O1 tool steel in wire-cut EDM using robust design and desirability approach. *Int. J. Adv. Manuf. Technol.* **2019**, *103*, 2411–2422, doi:10.1007/s00170-019-03720-3.
29. Nawaz, Y.; Maqsood, S.; Naeem, K.; Nawaz, R.; Omair, M.; Habib, T. Parametric optimization of material removal rate, surface roughness, and kerf width in high-speed wire electric discharge machining (HS-WEDM) of DC53 die steel. *Int. J. Adv. Manuf. Technol.* **2020**, *107*, 3231–3245, doi:10.1007/s00170-020-05175-3.
30. Rehman, M.; Khan, S.A.; Naveed, R. Parametric optimization in wire electric discharge machining of DC53 steel using gamma phase coated wire. *J. Mech. Sci Technol.* **2020**, *34*, 2767–2773, doi:10.1007/s12206-020-0609-2.
31. Çardaklı, İ.S. *Thin Section High Cooling Rate Solidification, Thermomechanical Processing and Characterization of AISI DC53 Cold Work Tool Steel*; Middle East Technical University: Ankara, Turkey, 2019. Available online: https://open.metu.edu.tr/bitstream/handle/11511/45197/index.pdf (accessed on 31 March 2021).
32. Ishfaq, K.; Anwar, S.; Ali, M.A.; Raza, M.H.; Farooq, M.U.; Ahmad, S.; Salah, B. Optimization of WEDM for precise machining of novel developed Al6061-7.5% SiC squeeze casted composite. *Int. J. Adv. Manuf. Technol.* **2020**, doi:10.1007/s00170-020-06218-5.

33. Mughal, M.P.; Farooq, M.U.; Mumtaz, J.; Mia, M.; Shareef, M.; Javed, M.; Pruncu, C.I. Surface modification for osseointegration of Ti6Al4V ELI using powder mixed sinking EDM. *J. Mech. Behav. Biomed. Mater.* **2020**, 104145, doi:10.1016/j.jmbbm.2020.104145.
34. Umar Farooq, M.; Pervez Mughal, M.; Ahmed, N.; Ahmad Mufti, N.; Al-Ahmari, A.M.; He, Y. On the Investigation of Surface Integrity of Ti6Al4V ELI Using Si-Mixed Electric Discharge Machining. *Materials* **2020**, *13*, 1549, doi:10.3390/ma13071549.
35. Tosun, N.; Cogun, C.; Tosun, G. A study on kerf and material removal rate in wire electrical discharge machining based on Taguchi method. *J. Mater. Process. Technol.* **2004**, *152*, 316–322, doi:10.1016/j.jmatprotec.2004.04.373.
36. Mussada, E.K.; Hua, C.C. Rao AKP Surface hardenability studies of the die steel machined by WEDM. *Mater. Manuf. Process.* **2018**, *33*, 1745–1750, doi:10.1080/10426914.2018.1476695.
37. Somashekhar, K.P.; Ramachandran, N.; Mathew, J. Material removal characteristics of microslot (kerf) geometry in μ-WEDM on aluminum. *Int. J. Adv. Manuf. Technol.* **2010**, *51*, 611–626, doi:10.1007/s00170-010-2645-z.
38. Groover, M. *Fundamentals of Modern Manufacturing: Materials, Processes, and Systems*, 4th ed.; John Wiley & Sons, Inc.: Hoboken, NJ, USA, 2013; ISBN 978-0470467008.
39. Tilekar, S.; Das, S.S.; Patowari, P.K. Process Parameter Optimization of Wire EDM on Aluminum and Mild Steel by Using Taguchi Method. *Procedia Mater. Sci.* **2014**, *5*, 2577–2584, doi:10.1016/j.mspro.2014.07.518.
40. Farooq, M.U.; Ali, M.A.; He, Y.; Khan, A.M.; Pruncu, C.I.; Kashif, M.; Asif, N. Curved profiles machining of Ti6Al4V alloy through WEDM: Investigations on geometrical errors. *J. Mater. Res. Technol.* **2020**, *9*, 16186–16201, doi:10.1016/j.jmrt.2020.11.067.
41. Ishfaq, K.; Farooq, M.U.; Anwar, S.; Ali, M.A.; Ahmad, S.; El-Sherbeeny, A.M. A comprehensive investigation of geometrical accuracy errors during WEDM of Al6061-7.5% SiC composite. *Mater. Manuf. Process.* **2020**, *36*, 362–372, doi:10.1080/10426914.2020.1832683.
42. Asad, A.M.; Kashif, I.; Raza, M.H.; Umar, F.M.; Mufti, N.A.; Pruncu, C.I. Mechanical characterization of aged AA2026-AA2026 overcast joints fabricated by squeeze casting. *Int. J. Adv. Manuf. Technol.* **2020**, *107*, 3277–3297.